PERGAMON

International Journal of Heat and Mass Transfer 42 (1999) 4027–4041

International Journal of HEAT and MASS TRANSFER

www.elsevier.com/locate/ijhmt

Second law analysis of a swirling flow in a circular duct with restriction

B.S. Yilbas*, S.Z. Shuja, M.O. Budair

Mechanical Engineering Department, KFUPM, Dhahran 31261, Saudi Arabia

Received 1 January 1998

Abstract

The present study is conducted to examine the entropy generation and second law analysis for the laminar flow passing through a circular duct with restriction and swirl. The governing fluid and energy equations are solved numerically for the combination of the conditions of restriction and swirling. The dimensionless quantities for the entropy generation, heat transfer and irreversibility are developed. The influence of Prandtl number, restriction and swirl on the dimensionless quantities and merit number are discussed. It is found that the irreversibility increases with increasing Prandtl number. The effect of swirling and restriction on the dimensionless quantities is more pronounced at high Prandtl numbers.

1. Introduction

The viscous flows through ducts with symmetric sudden contractions in cross-sectional area results in flow field that may be of interest in many engineering areas. A number of studies have been carried out introducing different contraction ratios [1,2]. Many aspects of axisymmetric flow in contractions were discussed that encompasses Newtonian and non-Newtonian viscoelastic fluids [3]. The velocity field developed due to flow through an abrupt contraction and expansion was investigated by Xia et al. [4]. They demonstrated that the Reynolds number associated with the inlet flow condition was the determining factor for the flow field development.

The transitional flow and its convective heat transfer in a smooth pipe were examined by Huiren and Songling [5]. They showed that in the fully developed region, flow and heat transfer were not affected by inlet turbulence intensities. Conjugate heat transfer in a thick-walled pipe with developing laminar flow was investigated by Schutte et al. [6]. They considered two transient situations, which included the transient heat transfer in steady, developing pipe flow, and the simultaneous transient development of flow and heating in a pipe. They concluded that all the parameters considered had significant influence on the Nusselt number, interfacial temperature, bulk temperature, and interfacial heat flux. The steady conjugate heat transfer in a developing pipe flow was numerically investigated by Faghri et al. [7]. They considered a blowing and suction at the inner pipe wall in heat pipes. Yan et al. [8] investigated the conjugate heat transfer in fully developed pipe flows when the pipe wall temperature was suddenly raised to a new constant temperature.

On the other hand, the optimal design for thermal systems may rely on the minimization of the entropy generation in the system. In recent years, entropy minimization has become a topic of great interest in the thermo-fluid area. In fluid flow, the irreversibility arises due to the heat transfer and the viscous effects of the

* Corresponding author. Tel.: +966-3-860-2540; fax: +966-3-860-2949.

E-mail address: factme@saupm00.bitnet (B.S. Yilbas)

0017-9310/99/$ - see front matter
PII: S0017-9310(99)00066-6

Nomenclature

A_P	coefficient for ϕ in the numerical expression
a	area
D	duct diameter
$d\theta$	angular increment
E	Eckert number
h	enthalpy
I	irreversibility
I^*	dimensionless irreversibility
k	thermal conductivity
L	length of duct
M	merit number
$\dot{m}$	mass flow rate
Pr	Prandtl number
P	pressure
Q	heat transfer
Q^*	dimensionless heat transfer
R	radius of the duct
Re	Reynolds number
r	distance in the radial direction
S_ϕ	source term for variable ϕ
S'''^*	volumetric dimensionless entropy generation
S'''_{gen}	volumetric entropy generation
$\overline{S'''_{gen}}^*$	volumetric averaged dimensionless entropy generation
T	temperature
T_a	ambient or reference temperature
T_w	temperature at the wall
$\forall$	volume
V	velocity in the radial direction
W	velocity in the axial direction

Greek symbols

Γ_ϕ	exchange coefficient for ϕ
μ	dynamic viscosity
ρ	density (function of temperature and pressure for gas)
σ	temperature ratio (T_w/T)
Φ	viscous dissipation
ϕ	arbitrary variable

fluid. In the fluid system, when both temperature and velocity fields are known the entropy generation due to both effects at each point in the system can be predicted. The analytical solutions of the entropy generation for the developing and the fully developed flows within a smooth channel were obtained by Bejan [9] and Carrington and Sun [10]. The analytical approach to the problem however, becomes difficult as the geometric and flow conditions are complicated. Consequently, numerical solution to the problem becomes inevitable. Numerical predictions of entropy generation for mixed convective flow in a vertical channel with transverse fin array was investigated by Cheng and Ma [11]. They computed the local entropy generation by solving the entropy generation equation and they proposed a geometric configuration of the finned channel with improved second-law efficiency. An extensive review on entropy generation minimization was carried out by Bejan [12]. The review traced the development and adoption of the method in several sectors of mainstream thermal engineering and science. Thermodynamic analysis of convective heat transfer in a packed duct with asymmetrical wall temperatures was investigated by Demirel and Al-Ali [13]. They estimated the pressure drop due to packing and demonstrated the influence of physical and geometric parameters on the entropy generation. The second-law analysis of heat transfer in swirling flow through a cylindrical duct was investigated by Mukherjee et al. [14]. They calculated the local Nusselt number and rate of entropy generation. A merit function was defined and influence of swirling on the merit function was discussed. However, the study was limited to a cylindrical smooth duct, and the influence of Prandtl number on the entropy generation and the merit function was not discussed in detail. Consequently, the influence of restriction in swirling flow through a cylindrical duct and the effect of Prandtl number on the entropy generation need to be examined further.

In the present study, swirling flow through a cylindrical duct with restriction is taken into account. The wall temperature of the duct is considered as uniform and higher than the fluid temperature. The flow conditions are set to obtain a laminar case. Three-dimensional governing flow and energy equations are solved numerically introducing the control volume approach. Non-dimensional entropy generation, heat transfer, irreversibility and the merit function are derived. The effect of swirling and Prandtl number on the non-dimensional entropy generation, heat transfer, irreversibility and merit function are investigated.

2. Mathematical analysis

2.1. Flow and energy equations

The set of partial differential equations governing a

Table 1
Variables and the corresponding conservation equations

Conservation of	ϕ	Γ_ϕ	S_ϕ
Mass	1	0	0
Axial momentum	W	μ	$-\frac{\partial p}{\partial z}+\frac{\partial}{\partial z}(\mu\frac{\partial U}{\partial z})+\frac{1}{r}\frac{\partial}{\partial r}(r\mu_e\frac{\partial V}{\partial z})$
Radial momentum	V	μ	$-\frac{\partial p}{\partial r}+\frac{\partial}{\partial z}(\mu\frac{\partial W}{\partial z})+\frac{1}{r}\frac{\partial}{\partial r}(r\mu\frac{\partial V}{\partial r})-2\mu\frac{V}{r^2}+\rho\frac{U^2}{r}$
Tangential momentum	U	μ	$-(\frac{\mu}{r^2}+\rho\frac{V}{r}+\frac{1}{r}\frac{\partial\mu}{\partial r})U$
Enthalpy	h	μ/σ_h	$\mu\Phi$

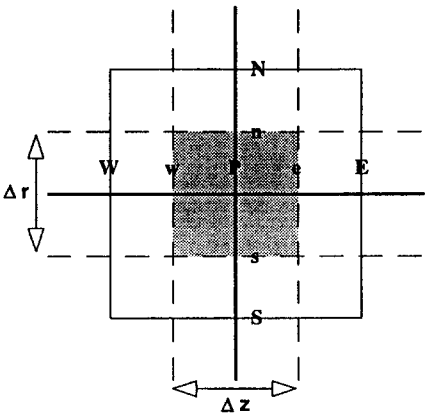

(a)

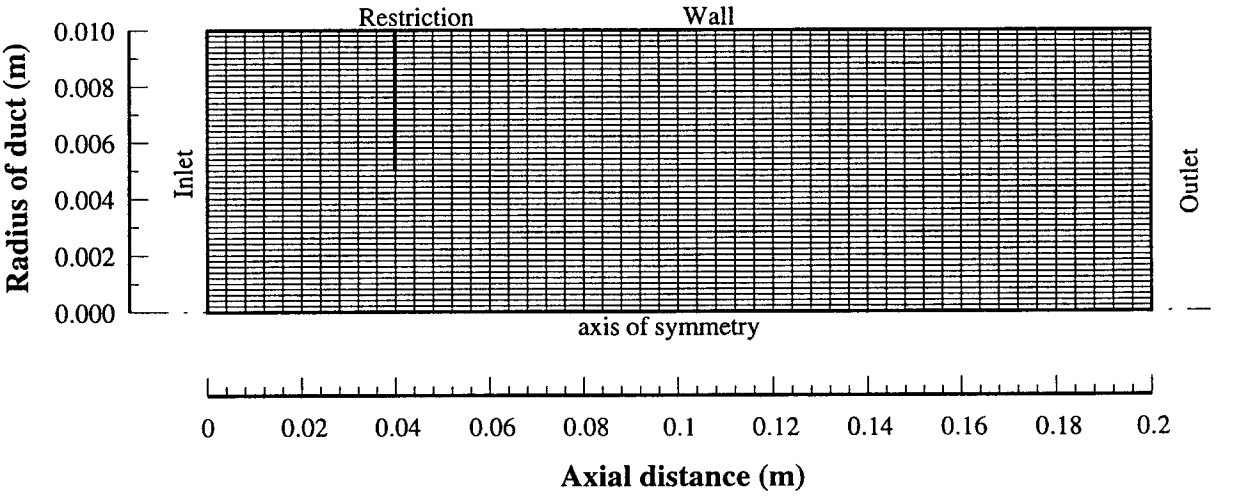

(b)

Fig. 1. Schematic view of (a) a two-dimensional grid and (b) grid used in the present computation.

steady flow field with constant swirl can be written in cylindrical polar coordinates (r, θ, z) as:

$$\frac{\partial}{\partial z}\left(\rho U\phi - \Gamma_\phi \frac{\partial \phi}{\partial z}\right) + \frac{1}{r}\frac{\partial}{\partial r}\left(\rho r V\phi - \Gamma_\phi r \frac{\partial \phi}{\partial r}\right) = S_\phi \quad (1)$$

In Eq. (1), ϕ is a general variable, Γ_ϕ is the exchange coefficient for the property ϕ, S_ϕ is the source expression for ϕ. In the most general form, it may comprise a term for the rate of generation of ϕ per unit volume together with other terms that cannot be included in terms on the left-hand side of Eq. (1).

Eq. (1) becomes the conservation for mass, z-momentum, r-momentum, θ-momentum and energy equations when setting $\phi = 1$, W, V, U and T respectively. Eq. (1) is the compactly represented elliptic partial differential equation, and the list of the dependent variables and the associated definitions of Γ_ϕ and S_ϕ are given in Table 1.

2.2. Boundary conditions

The boundary conditions appropriate to laminar flow through a circular duct (Fig. 1) with constant swirl, uniform wall temperature, and without and with restrictions are:

Without restriction:

At inlet:

$V = U =$ specified; $T =$ specified $= 300$ K

At wall

$W = V = U = 0$; $T =$ specified $= 400$ K

(constant along the pipe length)

At symmetry axis:

$$\frac{\partial W}{\partial r} = 0; \quad V = 0; \quad \frac{\partial T}{\partial r} = 0$$

At outlet:

$$\frac{\partial \phi}{\partial z} = 0$$

where ϕ represents a general variable.

With restriction

All the boundary conditions introduced for the case of without restrictions are applicable, and the following boundary conditions are imposed at the restriction:

$$\text{At } z = \frac{1}{5}L \quad \text{and} \quad 0 \le r \le \frac{D}{4}; \quad W = 0$$

where L is the duct length and D is the duct diameter.

2.3. Entropy, irreversibility and heat transfer analysis

The non-equilibrium process of exchange and momentum transfer within the fluid and at the solid boundaries results in continuous entropy generation in the flow system. The local entropy generation per unit volume for a incompressible newtonian fluid may be written as [15]:

$$S'''_{\text{gen}} = \frac{k}{T^2}(\nabla T)^2 + \frac{\mu}{T}\Phi \quad (2)$$

or $(S'''_{\text{gen}})_{\text{cond}} = k/T^2(\nabla T)^2$ and $(S'''_{\text{gen}})_{\text{fric}} = (\mu/T)\Phi$ where in polar coordinates;

$$\Phi = 2\left[\left(\frac{\partial V}{\partial r}\right)^2 + \left(\frac{V}{r}\right)^2 + \left(<\frac{\partial W}{\partial z}\right)^2\right] + \left(\frac{\partial U}{\partial z}\right)^2 + \left(\frac{\partial V}{\partial z} + \frac{\partial W}{\partial r}\right)^2 + \left(\frac{\partial U}{\partial r} - \frac{U}{r}\right)^2$$

Here, $(S'''_{\text{gen}})_{\text{cond}}$ represents the entropy generation per unit volume due to heat transfer and the $(S'''_{\text{gen}})_{\text{fric}}$ is the entropy generation per unit volume due to fluid friction.

S'''_{gen} can be written in non-dimensional form. In this case, the temperature is non-dimensionalized by dividing the wall temperature (T_w), spatial length is divided by the pipe radius (R) and the velocities are divided by the axial velocity (W). The resulting non-dimensional entropy generation per unit volume becomes:

$$S'''^{*}_{\text{gen}} = \frac{S'''_{\text{gen}} R^2}{k} = \sigma^2(\nabla T^*)^2 + Pr\, E\sigma(\Phi^*) \quad (3)$$

where $\sigma = (T_w/T)$ (T_w is the wall temperature), Pr is the Prandtl number ($\text{Pr} = \mu C_p/k$), and E is the Eckert number ($E = \omega_i^2/(C_p T_w)$, where W_i is the axial velocity at pipe inlet).

The volumetric averaged dimensionless entropy generation can be written as:

$$\overline{\dot{S}^*_{\text{gen}}} = \frac{1}{\forall}\int_{\forall} \frac{S'''_{\text{gen}} R^2}{k} \mathrm{d}\theta\, \mathrm{d}z\, r\, \mathrm{d}r$$

However, the irreversibility is defined as:

$$I = T_a \dot{S}_{\text{gen}}$$

where

$$\dot{S}_{gen} = \int_{\forall} \dot{S}'''_{gen} d\theta\, dz\, r\, dr$$

The combination of irreversibility with volumetric averaged dimensionless entropy generation results in:

$$I = T_a \overline{\dot{S}_{gen}}^{*} \frac{k}{R^2} \forall$$

or

$$I^* = \frac{I}{T_w} \frac{R^2}{k} \frac{1}{\forall} = \frac{T_a}{T_w} \overline{\dot{S}_{gen}}^{*} \tag{4}$$

where I^* is the non-dimensional irreversibility.

The heat transfer to the fluid can be written as:

$$Q = \dot{m} C_p (T_{exit} - T_{inlet}) = \dot{m}_{inlet} C_p \left[\frac{\dot{m}_{exit}}{\dot{m}_{inlet}} T_{exit} - T_{inlet} \right]$$

where $\dot{m}_{inlet} = \rho_i W_i A_i$ or

$$\frac{QR^2}{T_w k \forall} = Pr\, Re \frac{R}{2L} \left(\frac{T_{inlet}}{T_w} \right) \left[\frac{\dot{m}_{exit} T_{exit}}{\dot{m}_{inlet} T_{inlet}} - 1 \right]$$

or

$$Q^* = \frac{QR^2}{T_w k \forall}$$

$$= Pr\, Re \frac{R}{2L} \left(\frac{1}{\sigma} \right) \left[\frac{\left(\int_0^R \rho T\, d\theta\, dz\, r\, dr \right)_{exit}}{\left(\int_0^R \rho T\, d\theta\, dz\, r\, dr \right)_{inlet}} - 1 \right] \tag{5}$$

where Q^* is the non-dimensional heat transfer to the fluid. The rate of exergy transfer accompanying energy transfer at the rate of Q is given as [14]:

$$Q_a = Q \left(1 - \frac{T_a}{T_w} \right)$$

where T_a is the ambient or reference temperature, which is considered exergy reference environment temperature and T_w is the wall temperature which is considered as a suitable temperature at the surface where the heat transfer takes place.

The merit function is defined as the ratio of exergy transferred to the sum of exergy transferred and exergy destroyed [14], i.e.:

$$M = \frac{Q_a}{Q_a + I}$$

or using non-dimensional quantities:

$$M = \frac{Q^* \left(1 - \frac{T_a}{T_w} \right)}{Q^* \left(1 - \frac{T_a}{T_w} \right) + I^*} \tag{6}$$

3. Numerical solution of governing equations

The set of partial differential conservation equations governing the flow field are compactly presented by Eq. (1) and the accompanying Table 1, which lists the dependent variables and the associated definitions Γ_ϕ and S_ϕ. For the purpose of solution the flow domain is overlaid with a rectangular grid as shown in Fig. 1 whose intersection points (nodes) denote the location at which all variables, with the exception of the velocities, are calculated. The latter are computed at locations midway between the pressure which drive them. The details of the grid cluster are given in [16]. The mesh used in the present study has 2500 (50 × 50) node points as shown in Fig. 1.

The control volume approach is used in the numerical scheme. In this case Eq. (1) is integrated over the control volume, with the aid of assumptions about the relations between the nodal values at ϕ and the rates of creation/destruction of this entity within the cells and its transport by convection and diffusion across the cell boundaries. The former is represented in linearized form as:

$$S_\phi \equiv \int_{\forall} s_\phi\, d\forall = S_0 + S_P \phi_P$$

and the transport by expressions of the form e.g.:

$$\rho U_w \frac{(\phi_P + \phi_W)}{2} a_w - \Gamma_{\phi,w} \frac{(\phi_P + \phi_W)}{\delta x_{PW}} a_w$$

when the quantity Pe_w (the cell Peclet number$= \rho U_w \delta x_{PW} / \Gamma_{\phi,w}$) is small and by

$$\rho U_w \phi_W \quad \text{if} \quad U_w > 0$$

$$\rho U_w \phi_P \quad \text{if} \quad U_w < 0$$

when Pe_w is large in magnitude. Subscripts P and W refer to the central and west nodes, respectively, and w denotes the intervening cell boundary. Assembly of the above and similar expressions for the remaining boundaries yield for the finite difference equation in the form:

$$(A_P - S_P)\phi_P = \sum_n A_n \phi_n + S_0$$

where Σ_n is the summation over the neighboring

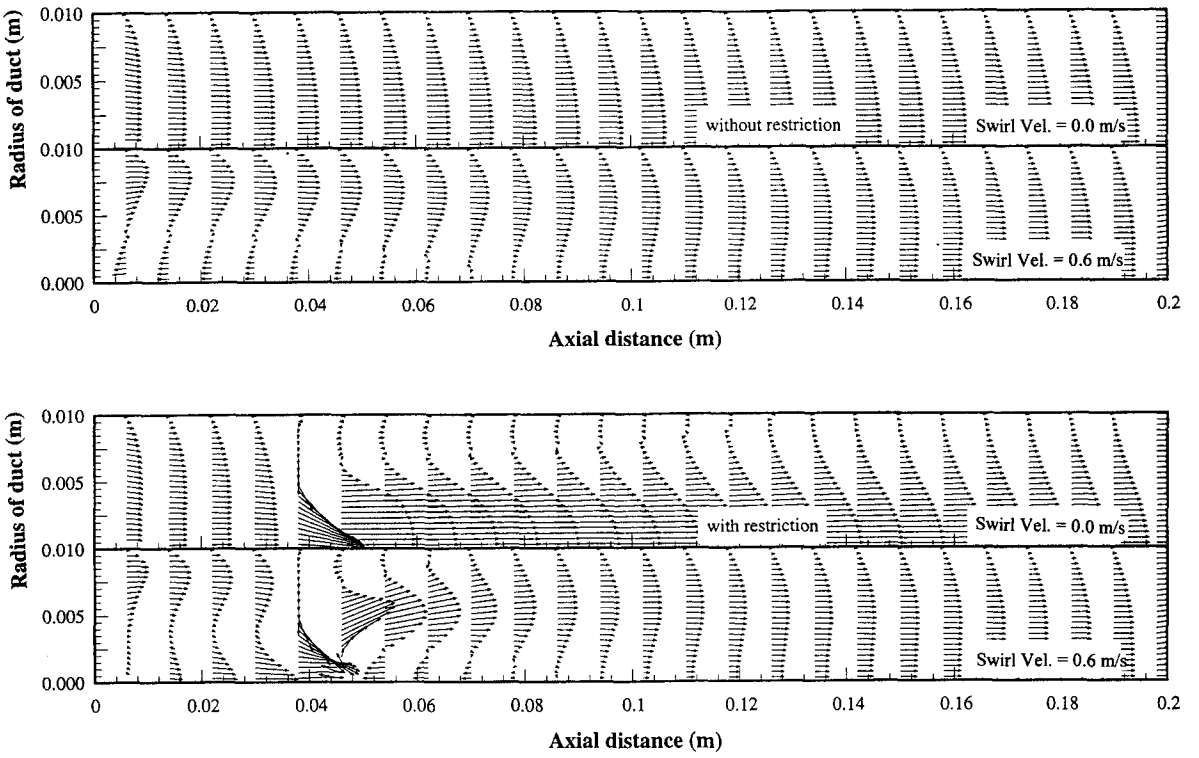

Fig. 2. Velocity vectors for the combination of cases of swirl and restriction.

nodes, $A_P = \Sigma A_n$, and S_0 and S_P are deduced from S_ϕ of Table 1. The finite difference equations are written for each of the variables at every cell with appropriate modifications being made to the total flux expressions at cells adjoining the boundaries of the solution domain to take account of the conditions imposed there. An equation for the unknown pressure is obtained by combining the continuity and momentum equations in the manner described in the literature [17].

A staggered grid arrangement is used in the present study. This arrangement provides handling the pressure linkages through the continuity equation and is known as the SIMPLE algorithm [18]. This method is an iterative process to steady-state convergence. The pressure link between continuity and momentum is accomplished by transforming the continuity equation into a Poisson equation for pressure. The Poisson equation implements a pressure correction for a divergent velocity field. The steady-state convergence is achieved by successively predicting and correcting the velocity components and the pressure. An initial guess for the pressure variable at each grid point is introduced.

4. Results and discussion

The numerical simulation of flow and temperature fields is carried out for various Prandtl numbers which range from 0.1 to 10, and swirl velocities ranging between 0 and 0.6 m/s. The results presented in the present study may be classified as the effect of restriction, Prandtl number and swirl velocities on the (i) flow field, (ii) entropy generation, and (iii) dimensionless heat transfer, irreversibility and merit function.

Fig. 2 shows the velocity vectors developed for smooth and restricted ducts with and without swirl conditions. In a smooth duct, flow develops as the axial distance increases. On the other hand, swirling results in reverse flow at the inlet region of the smooth duct (Fig. 2(a)). As the axial distance increases the flow disturbance due to swirling dies and the flow develops towards the duct end. In the case of restriction, the reverse flow is evident immediately after the restriction in the smooth duct. The reverse flow results in a considerably large recirculation region close to the solid boundary of the pipe. Flow recovers as the axial distance increases towards the end of the duct. Moreover, the effect of swirling on the flow field which

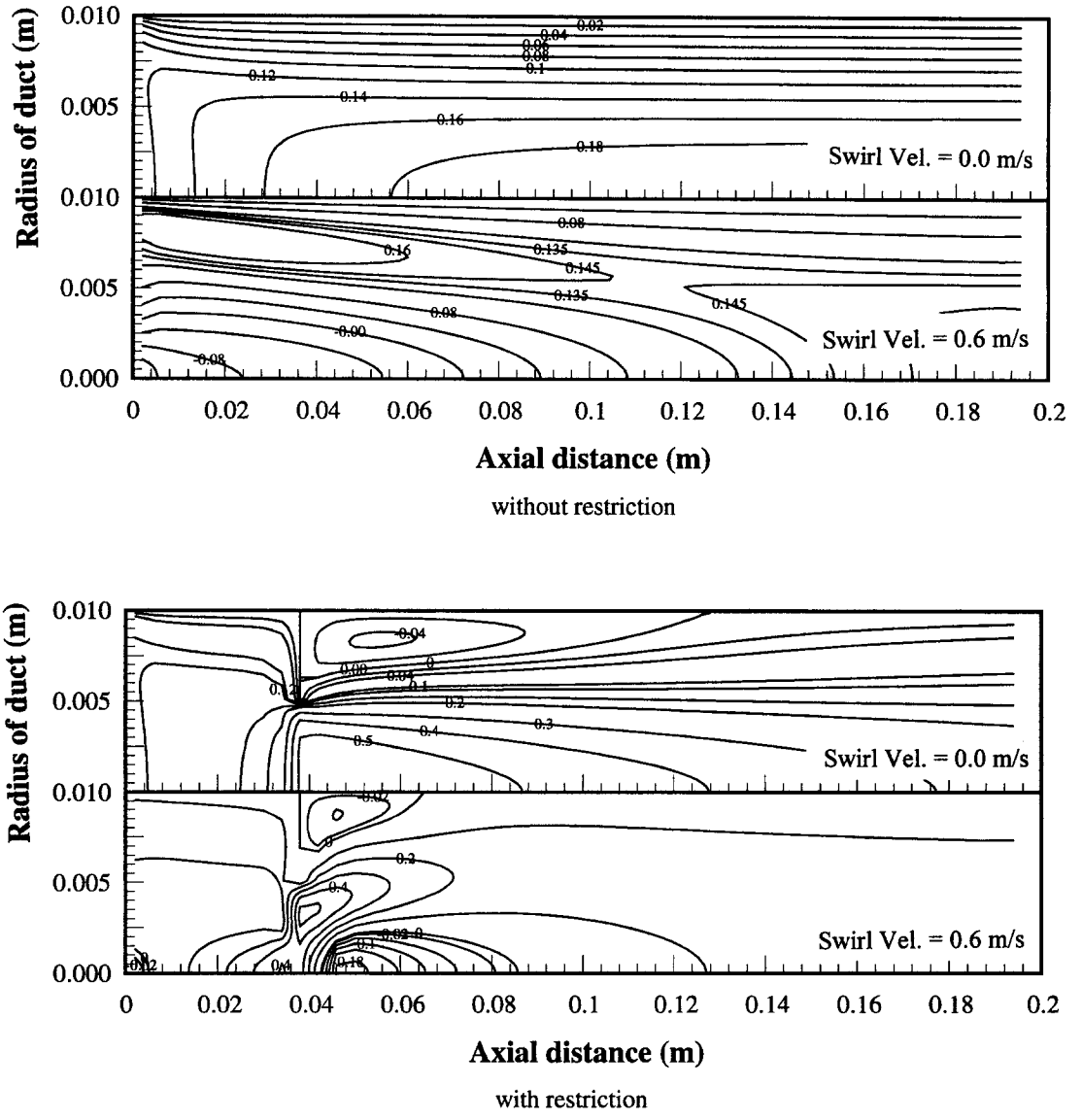

Fig. 3. Axial velocity (W) along the circular duct for the combination of cases of swirl and restriction.

is developed in the restricted duct, is more pronounced at the duct inlet and around the restricted region. In this case the flow at inlet first spills considerably upwards and develops an adverse effect on the flow close to the solid boundary. As the radial distance increases towards to the duct end, the reverse flow diminishes. When comparing swirling and no-swirling cases, the size of the circulation generated close to solid boundary after the restriction is larger in the case of no-swirling than that generated in the swirling case. In addition, the swirling generates a second recirculation region close to both the centerline of the duct and the restriction. When comparing both circulations generated due to swirling, the circulation generated close to the centerline is smaller than that which occurs close to the solid boundary of the duct. This may be due to the high kinetic energy of the fluid at the center line in which case the size of the circulation formed is reduced.

Fig. 3 shows the axial velocity (W) variation along the axial distance for smooth and restricted ducts with and without swirling conditions. In both cases, axial velocity increases as the axial distance increases. As indicated earlier, swirling results in a circulation formation in the region close to the inlet of the unrestricted duct. The axial velocity is slightly lesser in the

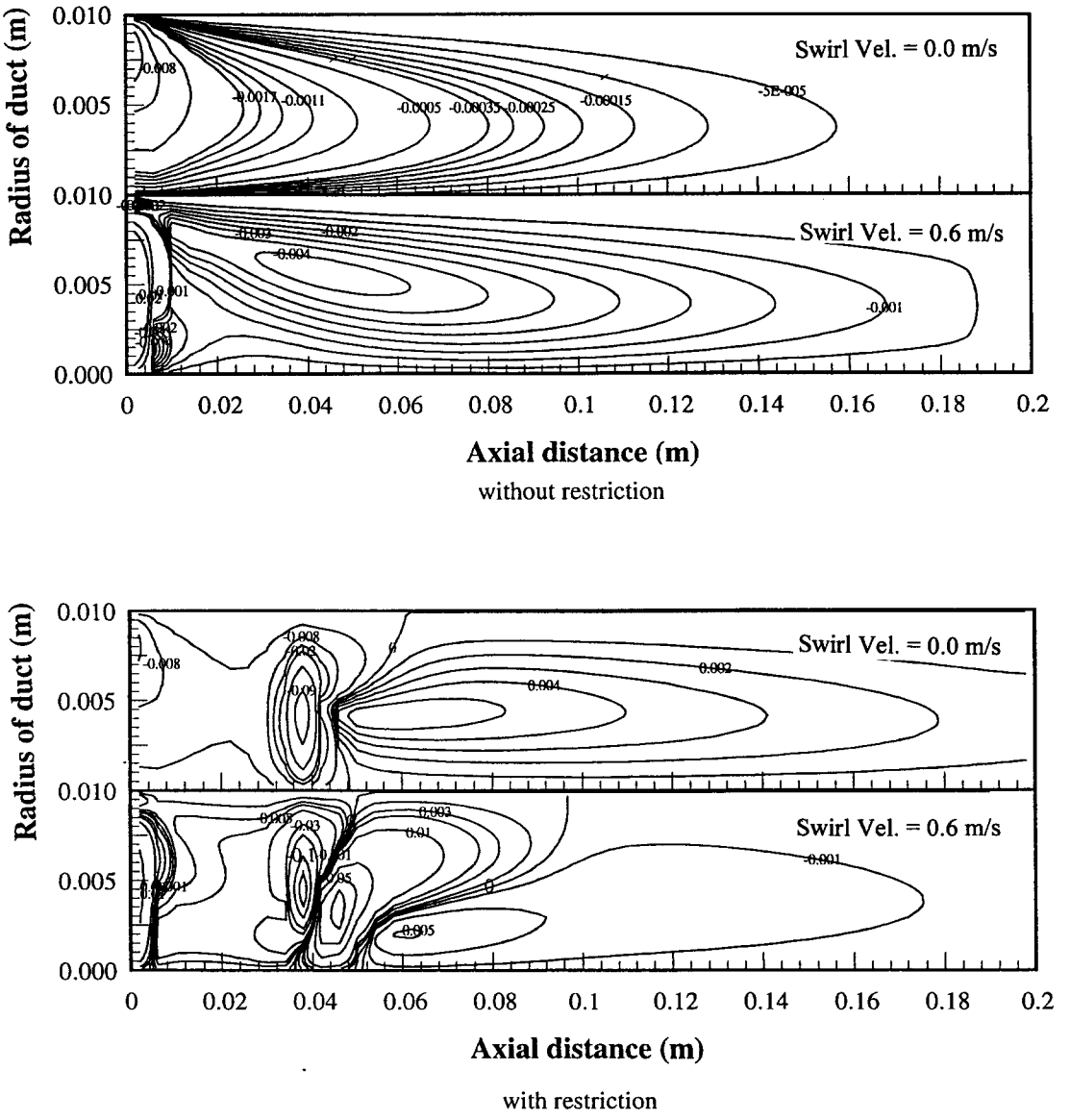

Fig. 4. Radial velocity (V) along axial distance for the combination of cases of swirl and restriction.

case of swirling than the no-swirling case. This may indicate that the development of the flow in the axial direction delays slightly when swirling is introduced. On the other hand, the restriction introduced in the duct disturbs the flow field considerably, which in turn results in a reverse flow and consequent circulation formation. In the case of no-swirling condition, a circulation is formed immediately after the restriction and close to the solid boundary. When the swirling is introduced, three circulations are seen close to the region of restriction.

Fig. 4 shows the radial velocity distribution along the axial distance for smooth and restricted ducts with and without swirling conditions. The flow attains parabolic velocity profiles, which develop as the axial distance increases for the smooth duct without swirling. As indicated before, swirling develops considerably large circulation after the duct inlet, which in turn disturbs the development of parabolic velocity profiles along the axial distance. The restriction, however, disturbs the flow resulting in formation of circulation regions. Moreover, the size of the circulations increase

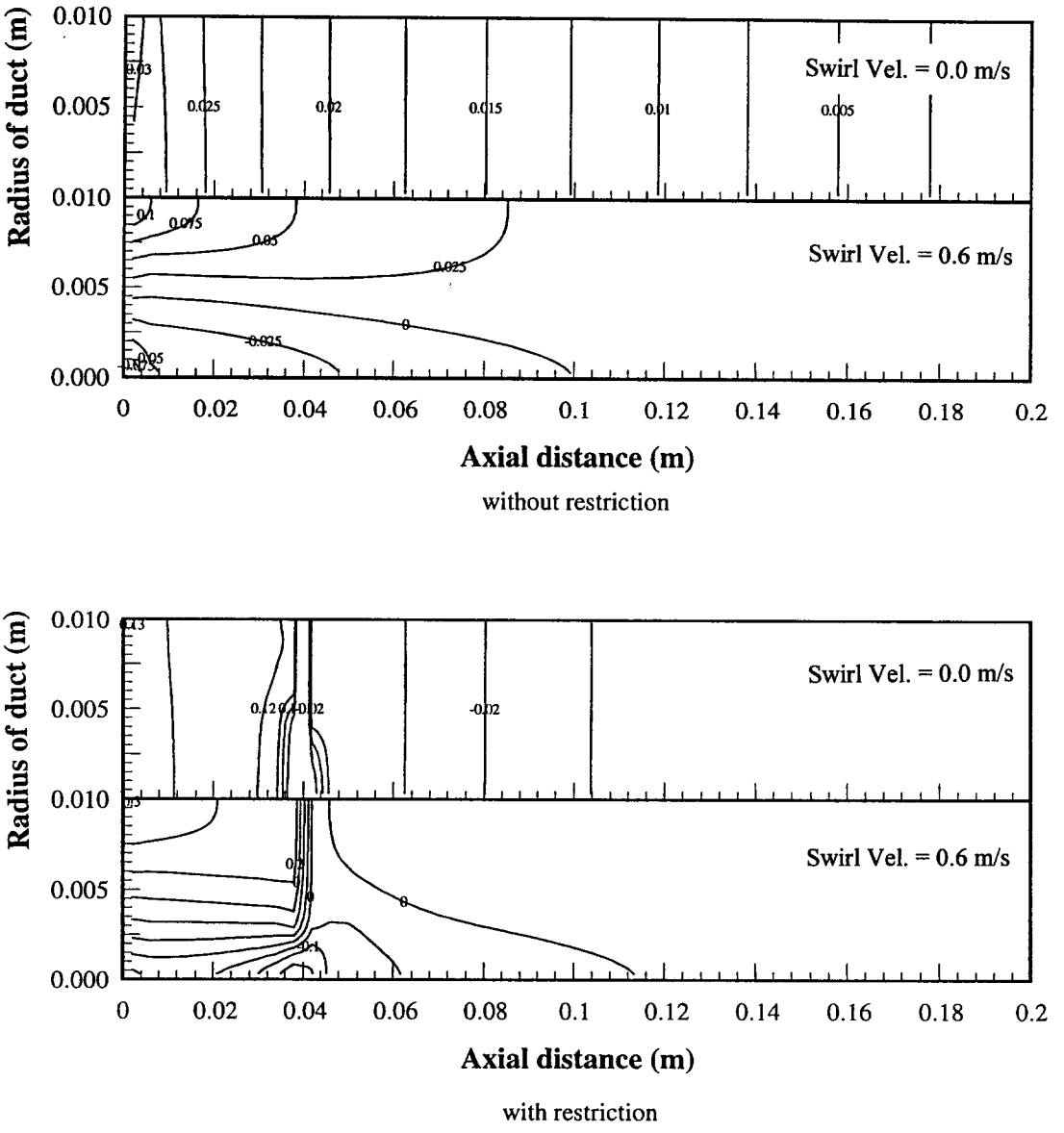

Fig. 5. Iso-bars along the circular duct axis for the combination of cases of swirl and restriction.

as the swirling is imposed. In this case, the circulation developed in the radial direction extends towards the center of the duct.

Fig. 5 shows the isobars for smooth and restricted ducts with and without swirling conditions. The straight constant-pressure lines are observed along the axial distance for a smooth duct without swirl condition. The isobars are disturbed as the swirling introduced for both smooth and restricted ducts. High pressure regions are developed in the vicinity of the restricted region. This extends further towards upstream when the swirling is introduced for the restricted duct.

Fig. 6 shows the logarithm of the constant entropy generation lines, due to fluid friction and heat transfer, along the axial distance for smooth duct with and without swirl conditions. The entropy generated per unit volume due to fluid friction increases at the inlet and close to the solid boundary for both swirl and no-swirl conditions. This may be attributed to the flow distortion in which case, frictional loss increases substantially. When comparing swirl and no-swirl con-

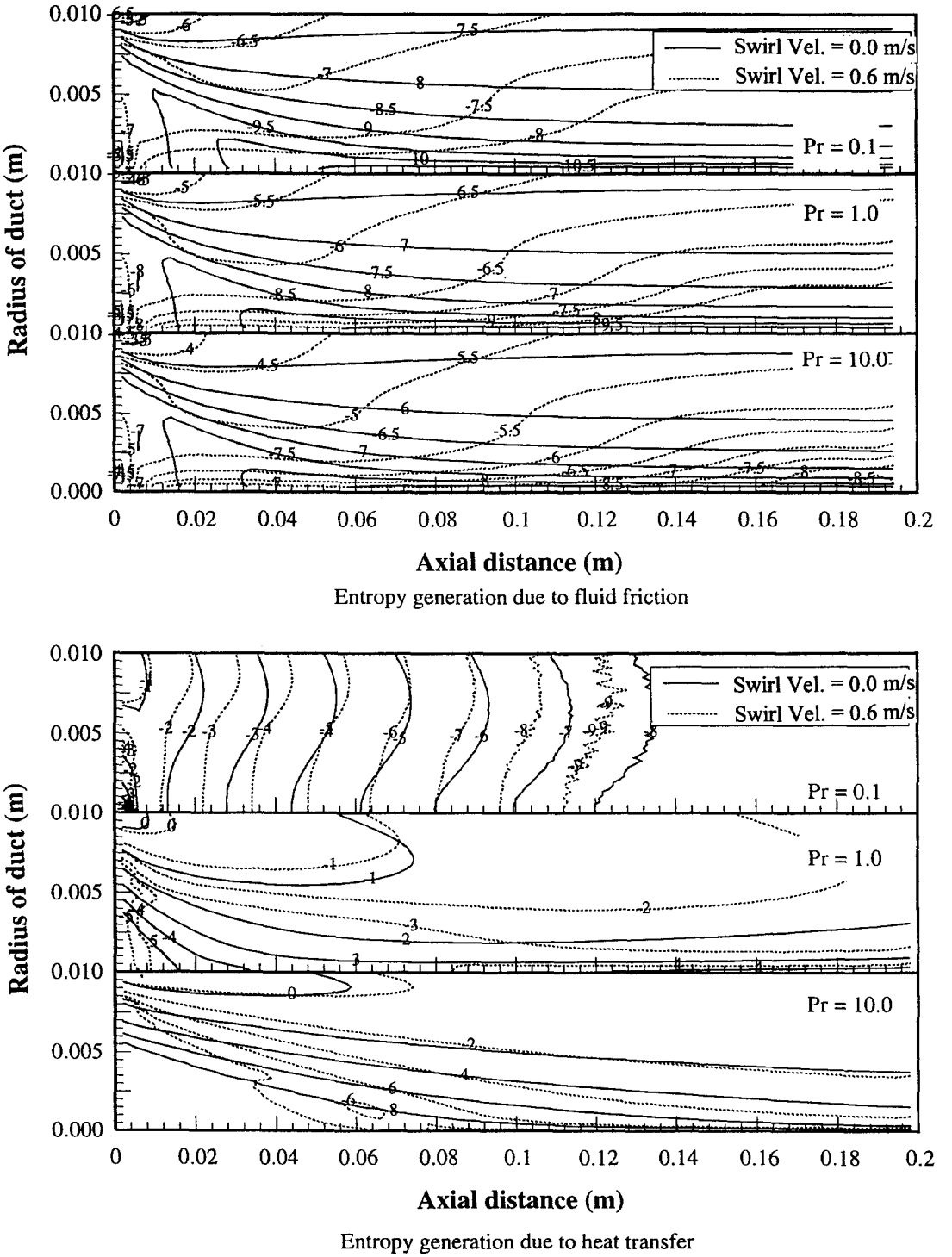

Fig. 6. Entropy generation contours due to fluid friction and heat transfer for flow in a duct without restriction. Variation for three Prandtl numbers and two swirl conditions.

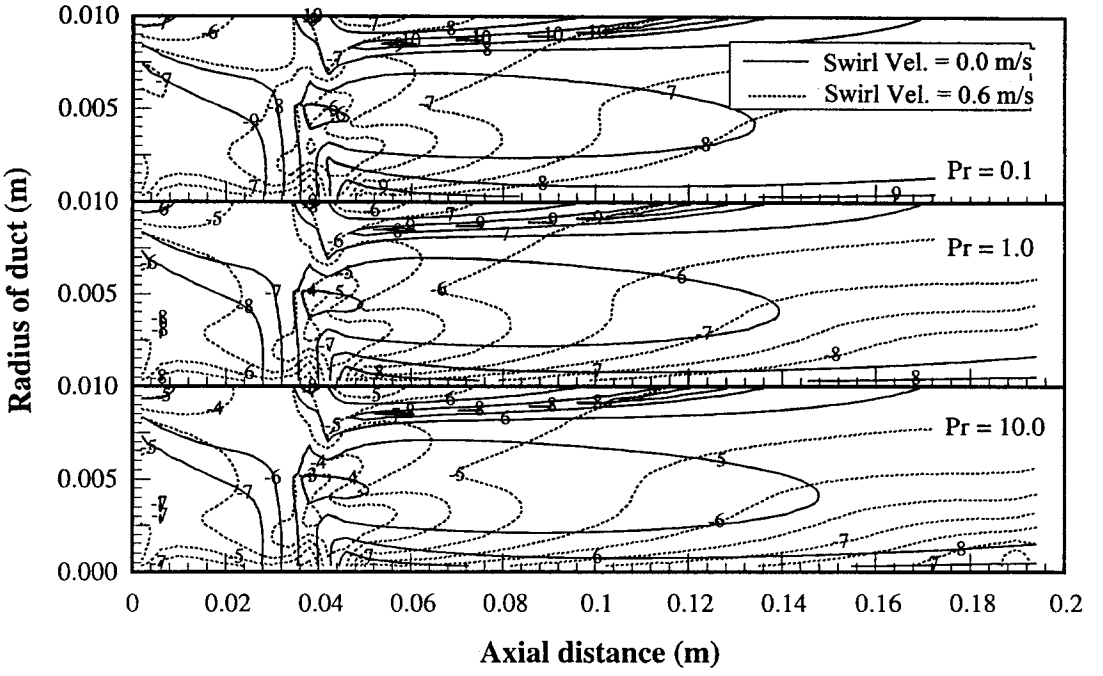

Entropy generation due to fluid friction

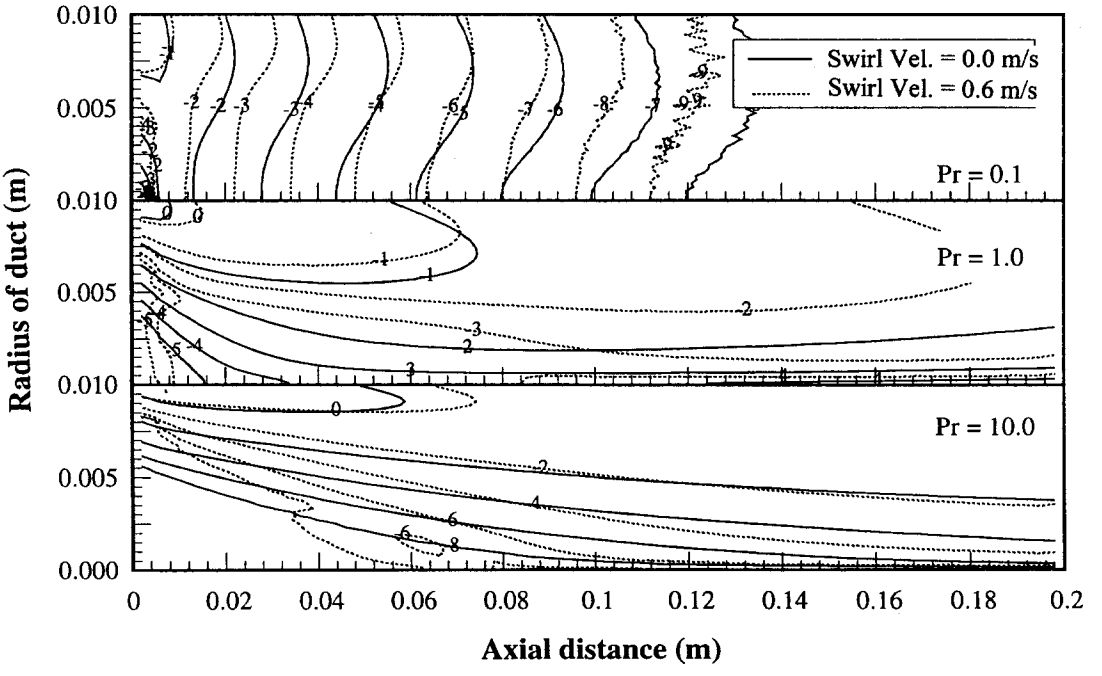

Entropy generation due to heat transfer

Fig. 7. Entropy generation contours due to fluid friction and heat transfer for flow in a duct with restriction. Variation for three Prandtl numbers and two swirl conditions.

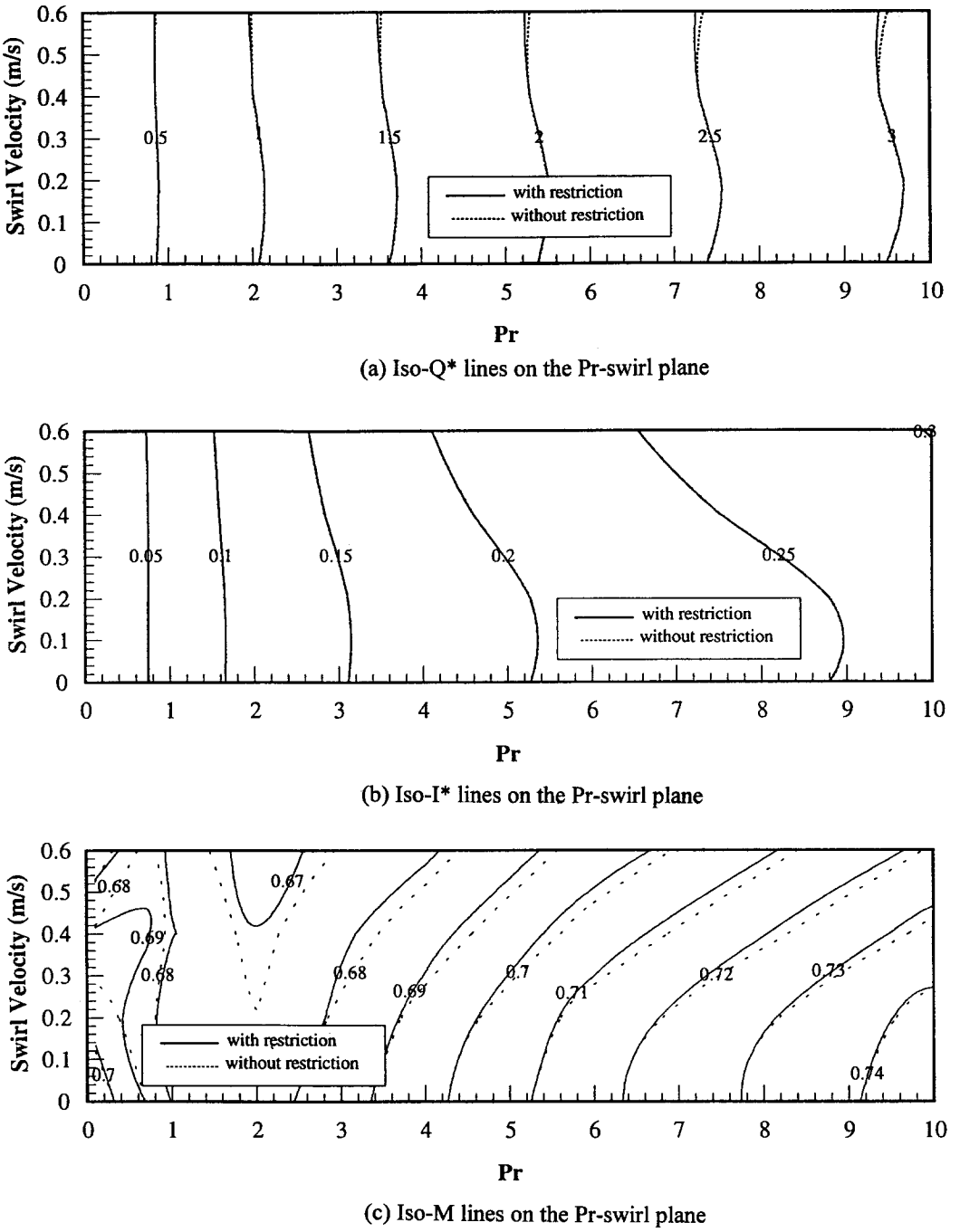

(a) Iso-Q* lines on the Pr-swirl plane

(b) Iso-I* lines on the Pr-swirl plane

(c) Iso-M lines on the Pr-swirl plane

Fig. 8. Contour plots for Q^*, I^* and M. Variation with Prandtl number and swirl velocity for the conditions of with and without restriction.

ditions, the effect of swirl on the entropy generation is apparent i.e. the entropy generation increases in the case of swirling. However, the influence of Pr on the frictional entropy generation is insignificant. On the other hand, entropy generation due to heat transfer differs significantly from the frictional entropy generation; in this case, frictional entropy generation attains considerably lower values as compared to entropy generation due to heat transfer. This may be because of the temperature difference between the solid boundary

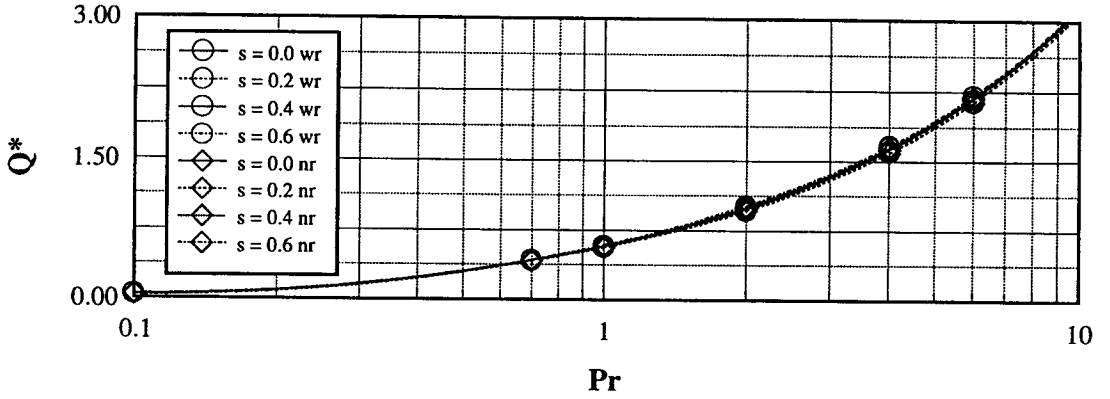

(a) Non-dimensional Heat transfer

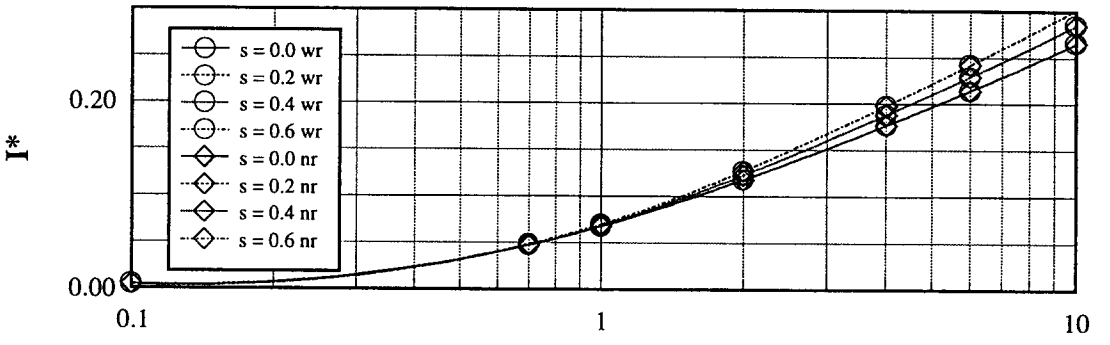

(b) Non-dimensional Irreversibility

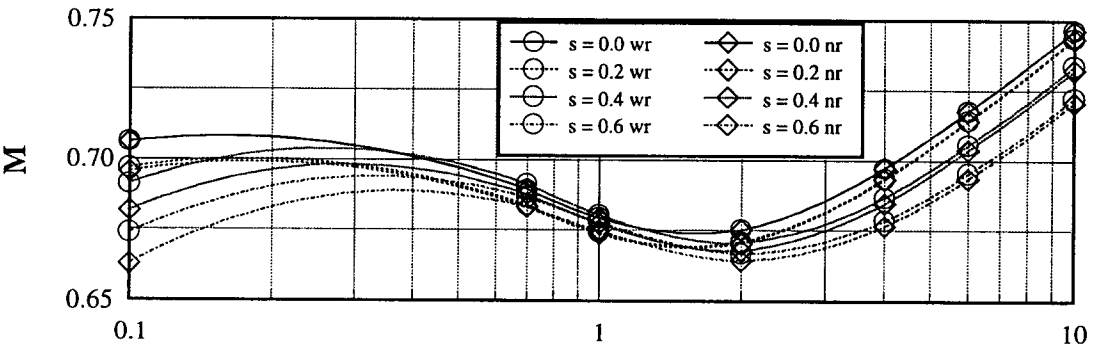

(c) Merit number

Fig. 9. Variation of Q^*, I^* and M with Prandtl number for the combination of cases of swirl and restriction. s, wr and nr represent swirl velocity (m/s), with restriction and no-restriction, respectively.

and the fluid inlet temperature, which is 100°C. The effect of swirling is more pronounced at $Pr = 1$.

The entropy generation due to friction and heat transfer for restricted duct is shown in Fig. 7. The restriction results in considerable frictional entropy generation close to the restricted region and solid boundary. This may be due to the circulation formed in these regions. The constant entropy lines follow almost the velocity contours for the no-swirling case. As the swirling is imposed, the constant entropy lines become drift appearance close to the restriction region. However, once the flow is developed towards the duct end, constant entropy lines are straightened. The influence of the Pr on the entropy generation due to heat transfer is similar to that occurred in Fig. 6. In this case, the effect of restriction on the entropy generation due to heat transfer is almost negligible. Moreover, the effect of Pr on the entropy generation is more pronounced at high Pr, as indicated earlier.

Fig. 8(a) shows the constant non-dimensional heat transfer (Q^*) lines with swirl velocity and Prandtl number for the conditions of with and without restrictions. Small variation occurs in iso-Q^* lines with swirl velocity at low Pr. As the Pr increases iso-Q^* lines deviate from the straight appearance. Therefore, the influence of the Pr on the Q^* becomes considerable at high swirl velocities. The effect of swirling on Q^* is significant as the Pr increases. In this case, the slope of iso-Q^* lines changes as the swirl velocity increases. In addition, the influence of restriction is more pronounced at high swirl velocities and Pr. Fig. 8(b) shows the constant-non-dimensional irreversibility (I^*) lines with swirl velocity and Pr for restriction and no-restriction conditions. Similar to Fig. 7, the influence of Pr and swirl velocities on the I^* is insignificant at low Pr. However, as Pr increases, I^* increases and the effect of swirl on the I^* becomes significant. In addition, the influence of restriction on iso-I^* lines is insignificant at low Pr. Fig. 8(c) shows the constant merit number (M) lines with swirl velocity and Pr for the conditions of with and without restriction. The iso-M lines have drift appearance at low Pr and high swirl velocities. As Pr and swirl velocity increase iso-M lines smoothens and inclines with positive slope. The influence of restriction is more pronounced when swirling velocity increases.

Fig. 9(a) shows the dimensionless heat transfer (Q^*) with Pr for the conditions of with and without restriction and swirl. Q^* increases with increasing Pr as consistent with the previous findings [14]. The effect of swirl and restriction may become visible at high Pr numbers, however, this effect is small. Therefore, it is the Pr that influences the heat transfer substantially as compared to swirling and restriction. Fig. 9(b) shows the dimensionless irreversibility (I^*) with Pr for the conditions with and without restriction and swirl. I^* increases as Pr increases. This may occur because of the entropy generation due to heat transfer and friction, provided that the contribution of frictional entropy generation to the irreversibility substantiates when the swirling and restriction are introduced. The effect of swirling and restriction on the I^* becomes apparent at high Pr. Fig. 9(c) shows the variation of merit number (M) with Pr at various combinations of conditions including restriction and swirling. M varies considerably with Pr such that it first increases and decreases to attain minimum, then increases with increasing Pr. This may be due to the fact that the increase in heat transfer is higher than the irreversibility increase for $0.3 < Pr < 2$. On the other hand, M increases and attains a positive slope for $2 < Pr < 10$. In this case the rate of increase in heat transfer well exceeds the rate of increase in irreversibility. The effect of swirl and restriction on M is more pronounced at high swirls and low Pr. The restriction and swirl reduces the M for all Pr, i.e. the lowest M is resulted at high swirl velocity. In addition, the point of minimum of M moves towards high Pr as the swirl velocity increases. Consequently, high swirl velocity may increase the heat transfer, but reduces the M because of the irreversibility generated.

5. Conclusions

The conclusions derived from the present work may be listed as follows:

1. The flow field is disturbed considerably when swirling and restrictions are imposed onto the flow in the duct. This results in circulation in the region close to the restriction and the solid boundary. Consequently, the entropy generation due to friction is amplified in these regions. On the other hand, the entropy generation as a result of heat transfer attains considerably higher values than that generated due to friction. The swirling and restriction enhance the entropy generation due to heat transfer. The effect of the Pr on the entropy generation is considerable. This effect is more pronounced at high Pr.
2. Non-dimensional heat transfer (Q^*) increases as Pr and the swirl velocity increase. The effect of swirl and restriction on Q^* may become apparent at high Pr provided that this effect is not substantiated as compared to the effect of Pr on Q^*.
3. Non-dimensional irreversibility (I^*) increases with increasing Pr. This may be the result of entropy generation due to heat transfer enhancement at high Pr. The effects of swirl velocity and the restriction on the I^* become significant as Pr increase.
4. Merit number (M) varies considerably as Pr

increases. M attains low values for $0.3 < Pr < 2$. Alternatively, M increases for $2 < Pr < 10$. Increase in M indicates that the rate of increase in heat transfer well exceeds the rate of increase in irreversibility. The effect of restriction and swirl velocity on M is visible at high swirl velocity and low Pr. The lowest M occurs when no-restriction and high swirl velocity are introduced. Therefore, high swirl velocity may increase the heat transfer, but reduces the M because of the attainment of high irreversibility.

References

[1] F. Drust, W.F. Schierholz, A.M. Wunderlich, Experimental and numerical investigations of plane duct flows with sudden contraction, Journal of Fluids Engineering 109 (1987) 376–383.

[2] F. Durst, T. Loy, Investigation of laminar flow in a pipe with sudden contraction of cross-sectional area, Computers and Fluids 13 (1) (1985) 15–36.

[3] D.V. Bager, Circular entry flows of inelastic and viscoelastic fluids. Advance in Transport Processes, II (1982).

[4] Y. Xia, P.T. Calloghan, K.R. Jeffrey, Velocity profiles: flows through an abrupt contraction and expansion, AIChE Journal 38 (9) (1992) 1408–1420.

[5] Z. Huiren, L. Songling, Numerical simulation of transitional flow and heat transfer in a smooth pipe, International Journal of Heat and Mass Transfer 34 (10) (1991) 2475–2482.

[6] D.J. Schutte, M.M. Rahman, A. Faghri, Transient conjugate heat transfer in a thick-walled pipe with developing laminar flow, Numerical Heat Transfer, Part A 21 (1992) 163–186.

[7] A. Faghri, M.M. Chen, E.T. Mahefkey, Simultaneous axial conduction in fluid and the pipe wall for forced convective laminar flow with blowing and suction at the wall, International Journal of Heat and Mass Transfer 32 (1989) 281–288.

[8] W.M. Yan, Y.L. Tsay, T.F. Lin, Transient conjugated heat transfer in laminar pipe flow, International Journal of Heat and Mass Transfer 32 (1989) 775–777.

[9] A. Bejan, A study of entropy generation in fundamental convective heat transfer, Journal of Heat Transfer 101 (1979) 718–725.

[10] C.G. Carrington, Z.F. Sun, Second law analysis of combined heat and mass transfer in internal flow and external flows, International Journal of Heat and Fluid Flow 13 (1) (1992) 65–70.

[11] H. Cheng, W. Ma, Numerical predictions of entropy generation for mixed convective flows in a vertical channel with transverse fin array, International Communications in Heat and Mass Transfer 21 (4) (1994) 519–530.

[12] A. Bejan, Entropy generation minimization: the new thermodynamics of finite-size devices and finite-time processes, Journal of Applied Physics 79 (3) (1996) 1191–1218.

[13] Y. Demirel, H. Al-Ali, Thermodynamic analysis of convective heat transfer in a packed duct with asymmetrical wall temperatures, International Journal of Heat and Mass Transfer 40 (5) (1997) 1145–1153.

[14] P. Mukherjee, G. Biswas, P.K. Nag, Second-law analysis of heat transfer in swirling flow through a cylindrical duct, Journal of Heat Transfer 109 (1987) 308–313.

[15] A. Bejan, Entropy Generation Minimization, CRC Press, New York, 1995.

[16] S.Z. Shuja, Calculations of fluid flow and heat transfer in expanding ducts, Master's thesis, King Fahd University of Petroleum and Minerals, Dhahran, Saudi Arabia, 1993.

[17] A.D. Gosman, E.E. Khalil, J.H. Whitelaw, The calculation of two-dimensional turbulent recirculating flows, in: F. Durst, B.E. Launder, F.W. Schmidt, J.H. Whitelaw (Eds.), Turbulent Sheat Flows I, Springer-Verlag, The Pennsylvania State University, New York, 1977, pp. 237–255.

[18] S.V. Patankar, Numerical Heat Transfer, McGraw-Hill, New York, 1980.